Metamaterial AMC backed Antenna for Body-worn Application at 2.45 GHz

Omisakin, Adedayo

Award date:
2017

Awarding institution:
Eindhoven University of Technology

Technische Universiteit
Eindhoven
University of Technology

Department of Electrical Engineering

Den Dolech 2, 5612 AZ Eindhoven
P.O. Box 513, 5600 MB Eindhoven
The Netherlands
http://w3.ele.tue.nl/nl/

Series title:
Master graduation paper,
Electrical Engineering

Commissioned by Professor:
Prof. dr. ir. Giampiero Gerini

Group / Chair:
Electromagnetics

Date of final presentation:
April 7, 2017

Report number:

(Optional for groups)

Metamaterial AMC backed Antenna for Body-worn Application at 2.45 GHz

by

Author: Adedayo Eberechukwu Omisakin

Internal supervisors: Asst. prof. dr. ir. Vito Lancellotti

External supervisors: ir. Mark Kleijnen, ir. Gert Doodeman

Metamaterial AMC backed Antenna for Body-worn Application at 2.45 GHz

Adedayo Omisakin
Department of Electrical Engineering
Eindhoven University of Technology
Eindhoven, The Netherlands
Email: a.e.omisakin@student.tue.nl

***Abstract*—Antennas worn on the human body for off-body communication suffer from impedance detuning, a significant drop in gain and efficiency due to the body degrading the antenna performance. An Artificial Magnetic Conductor (AMC), which is a type of metamaterial could shield the antenna from radiating towards the body, reducing the drop in gain and efficiency while having sufficient impedance bandwidth and good coverage. An AMC backed Coplanar fed Inverted-F Antenna (CPW-IFA) operating at the 2.45 GHz Industrial, Scientific and Medical (ISM) band was designed, simulated, fabricated and analyzed. The AMC was realized through a High Impedance Surface (HIS). A unit cell is designed and a 2×2 array was used to back the CPW-IFA and then optimized. Results show that the novel antenna is very robust to impedance detuning: the resonant frequency shifting more than 50 times less than the reference CPW-IFA when placed on the body. The simulated gain of 6.5 dBi and a 3 dB beamwidth of 86° show good coverage away from the body. The gain of the antenna, when placed on the body, dropped only by 0.8 dB while the radiation efficiency was 71% on the body. The compact 60 mm×60 mm×3.28 mm metamaterial backed antenna with a corresponding wavelength form factor of 0.5×0.5×0.027 is suitable for integration with wearable electronics.**

***Index Terms*—Metamaterial, Artificial Magnetic Conductor, High Impedance Surface, Body-worn antenna, CPW–IFA, off-body communication**

I. Introduction

Body-worn devices are on the rise for applications such as personal health monitoring and smartwatches. The antenna plays an important role in the performance of the communication system of a body-worn device. Two different applications can be distinguished: *on-body*, where both communicating devices are located on the same body, and *off-body* where only one of the communicating devices is located on a body. Both applications have different antenna performance requirements (gain, efficiency, impedance sensitivity, beamwidth). Figure 1 shows both off-body and on-body scenarios. When an antenna is placed on a human body the resonance frequency shifts (impedance detuning), the efficiency and gain drops, and the radiation pattern is distorted [1]. Also in body-worn antennas for off-body communication, radiation towards the body is undesired. This is in contrast to on-body communication where surface waves and coupling between antennas is exploited to improve antenna performance [2]. This paper is focused on improving the performance of body-worn antennas for off-body communication by using a metamaterial backing.

Fig. 1: Off-body and On-body communication

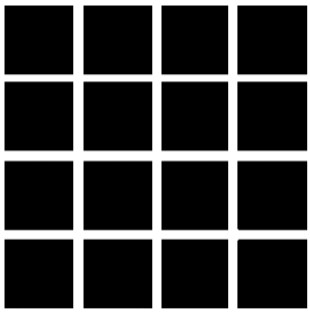

Fig. 2: A metamaterial surface (EBG, FSS or AMC)

Metamaterials are periodic structures that exhibit properties not readily found in nature such as negative refractive index [3], electromagnetic bandgap [4], frequency selectivity [5] and an artificial magnetic conductor [6], [7]. Figure 2 shows a metamaterial surface consisting of metallic patches and substrate beneath that could be engineered to realize either frequency selectivity, electromagnetic band gap or an artificial magnetic conductor. Metamaterials have been applied to antennas for various purposes. Electromagnetic bandgap structures (EBG) have been used to improve the bandwidth of patch antennas and suppress surface waves [8], [9], Frequency Selective Surfaces (FSS) have been used to improve the gain of antennas [10], Artificial Magnetic Conductor (AMC) have been used to realize low-profile antennas [11]. In this paper, an Artificial Magnetic Conductor is explored to improve the performance of body-worn antennas for off-body communication.

An Artificial Magnetic Conductor (AMC) is a class of metamaterial that has 0° reflection phase to an incident wave upon

its surface. This is in contrast to a Perfect Electric Conductor (PEC) that has $-180°$ reflection phase to an incident wave. The range of frequencies where the reflection phase is $0 \pm 90°$ is usually accepted as the AMC region and thus defined as its bandwidth. Figure 3 illustrates a PEC and an AMC very close to a radiator such as an antenna. When an antenna is backed with a metallic ground plane with a spacing less than $\lambda/4$, its $-180°$ reflection phase causes destructive interference to the forward propagating radiation, yielding poor return loss and in turn low total efficiency [12]. An AMC ground plane when engineered with a reflection coefficient of 1, could shield the body-worn antenna from being degraded by the human body, direct more radiation away from the body while maintaining good return loss and sufficient impedance bandwidth. If a PEC was used, it will require very thick substrates of about $\lambda/4$. In this work the AMC is realized through a High Impedance Surface (HIS).

In this paper, an AMC backed Coplanar-fed Inverted-F Antenna (CPW-IFA) operating at 2.45 GHz ISM band (2.4-2.5 GHz) is designed, manufactured and measured. Planar antennas such as patch antennas, printed dipoles and inverted-F antennas are well suited for body-worn applications due to their low cost, flexibility and ease of manufacture [13]. Co-planar fed antennas usually have a wider bandwidth than the conventionally fed ones [14], [15]. The Coplanar-fed Inverted-F Antenna (CPW-IFA) is designed and used as the reference antenna. This antenna is compact and has a wider bandwidth compared to other narrow band antennas such as a patch antenna. The CPW-IFA has only one layer followed by a substrate for mechanical support. An AMC through a High Impedance Surface is engineered and simulated in FEKO®. The AMC is used to back the CPW-IFA and optimized for the 2.45 GHz ISM band in CST Microwave Studio®. The novel antenna is fabricated and measured with and without a body phantom. The designed AMC backed antenna shows robustness to impedance detuning and a low drop in efficiency/ gain when placed directly on the human body, while providing a good coverage away from the body (beamwidth).

The remainder of this paper is a follows: In Section II, the theory and design of the AMC through a HIS is explained, Section III shows the performance of the designed reference antenna on the body highlighting the body-worn antenna challenge. Section IV presents the designed AMC backed antenna, its results and comparison with the reference antenna. In Section V, a parametric study is carried out on key design parameters. Section VI discusses the fabrication of the antenna, measurement and comparison with simulation.

II. Metamaterial: AMC through a HIS

A. Theory

A Perfect Electric Conductor (PEC) has $-180°$ reflection phase to an incident wave upon its surface. An AMC has $0°$ reflection phase to an incident wave upon its surface. The range of frequencies where the reflection phase is $0 \pm 90°$ is usually accepted as the AMC region and bandwidth. An AMC

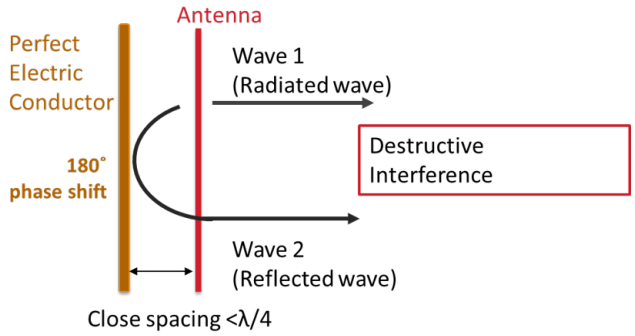

(a) PEC

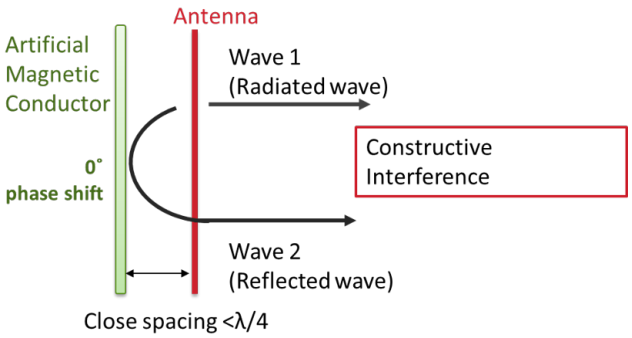

(b) AMC

Fig. 3: A radiator lying flat against a PEC and a Metamaterial AMC

can be realized through a High Impedance Surface (HIS). Let the surface impedance Z_S be:

$$Z_S = E_z/H_y \tag{1}$$

of a surface in the YZ plane. In a PEC the tangential electric field $E_t = 0$ so it follows from equation 1 that the surface impedance is zero. In contrast, in an AMC $H_t = 0$, thus the surface impedance is infinite. The $0°$ reflection phase in a HIS can be derived as follows: For a HIS in the yz-plane at x=0 Let

$$E(x) = E_f e^{-jkx} + E_b e^{jkx};\ H(x) = H_f e^{-jkx} + H_b e^{jkx} \tag{2}$$

represent the forward and backward TEM wave: where E(x), H(x) are the electric and magnetic field vector, E_f, H_f the foward travelling electric and magnetic field amplitudes and E_b, H_b the backward travelling electric and magnetic field amplitudes. Since the TEM wave has no electric and magnetic field components in its direction of propagation, equation 1 becomes:

$$Z_S = \frac{E_{total}(x=0)}{H_{total}(x=0)} \tag{3}$$

The ratio of the forward electric field to the forward magnetic field is the characteristic impedance of free space η:

$$\left|\frac{E_f(x)}{H_f(x)}\right| = \left|\frac{E_b(x)}{H_b(x)}\right| = \sqrt{\frac{\mu_0}{\epsilon_0}} = \eta \tag{4}$$

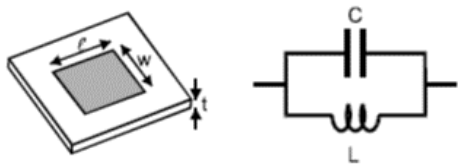

(a) Unit cell of the AMC (b) Simplified Equivalent circuit model

Fig. 4: An AMC (HIS) unit cell and Equivalent circuit model

The reflection phase relative to forward wave can be written as:

$$\Theta = \mathrm{Im}\left\{\ln\left(\frac{E_b}{E_f}\right)\right\} = \mathrm{Im}\left\{\ln\left(\frac{Z_S-\eta}{Z_S+\eta}\right)\right\} \quad (5)$$

From equation 5 when Z_S is high Θ= $0°$, which is the metamaterial AMC behavior.

Realizing a HIS is possible by engineering the structure shown in Figure 2. Figure 4a shows a unit cell of a potential HIS. It consists of a square metallic patch, a substrate and a metallic ground plane. Figure 4b shows its simplified equivalent circuit model. The capacitance C is caused by the proximity of the metal patch with the metal beneath, and also from the spacing between adjacent unit cells. The inductance L is the total self-inductance of the metal patch and its metal plane beneath. From the circuit model, the surface impedance can be expressed as:

$$Z_S = \frac{j\omega L}{1-\omega^2 LC} \quad (6)$$

If Z_S is high; i.e, $Z_S \longrightarrow \infty$ then $1-\omega^2 LC = 0$; it follows that the frequency at which that surface is a HIS and the reflection phase is $0°$ is given by :

$$\omega = 1/\sqrt{LC} \quad (7)$$

The fractional bandwidth can be approximated as [16]:

$$BW = \frac{\Delta\omega}{\omega} \sim \frac{1}{\eta}\sqrt{\frac{L}{C}} \quad (8)$$

From Figure 4a, l, w, and t are the length, width and thickness respectively. The inductance and capacitance of the structure have the following dependencies:

$$L \propto tl/w;\ C \propto \epsilon wl/t \quad (9)$$

where ϵ is the permivity of the substrate. the AMC frequency and bandwidth dependencies can be re-written as:

$$\omega \propto \frac{c}{\sqrt{\epsilon_r} l};\ BW \propto \frac{t}{\sqrt{\epsilon_r} w}. \quad (10)$$

where c is the speed of light in free space.

The dielectric constant and the size of the metallic patch are inversely proportional to the AMC frequency. While the thickness of the substrate layer is directly proportional to the bandwidth. The dielectric constant is inversely proportional to bandwidth. These concepts are used in designing the AMC behaviour at 2.45 GHz.

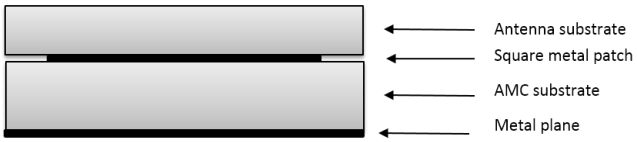

Fig. 5: Cross-section of the AMC unit cell (HIS plus the antenna substrate)

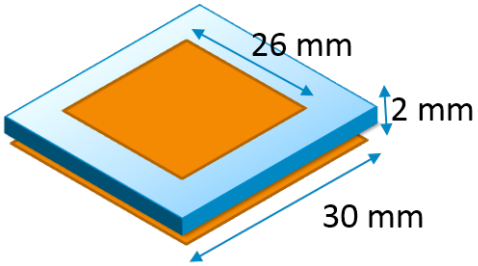

Fig. 6: Final Dimensions of the AMC unit cell

B. Design

A unit cell of the structure is simulated in FEKO® using periodic boundary conditions and an incident plane wave normal to surface ($\theta = 0; \phi = 0$) [17]. Figure 5 shows the cross-section of the HIS with the antenna substrate above. A unit cell size of about $\lambda/4$ is used and a side length of the square metallic patches is set to 25 mm. Practical dielectric constants within the range of 2 to 10.2 and a maximum thickness of 4 mm are investigated. The substrate above the AMC (Antenna substrate) was set to 1.2 mm and constrained to have the same dielectric constant of the substrate in the AMC for easy manufacturing. The structure is then designed to operate around 2.45 GHz. The final unit cell after design had an antenna substrate thickness of 1.2 mm, AMC substrate thickness of 2 mm, a dielectric constant of 4.2 for both substrates, a unit cell size of 30 mm and the side length of the metallic patches was 26 mm. Figure 6 shows the final dimensions of the AMC unit cell. Figure 7 shows the reflection phase diagram of an incident plane wave normal to the surface of the final unit cell along with the antenna substrate under periodic boundary conditions (infinitely peroidic). The 2.45 GHz ISM band is in the AMC region ($0\pm90°$). The magnitude of the reflection coefficient equals 1 for the entire frequency range because last layer is a PEC plane.

III. Reference Antenna Placed on the Body

In this section, the reference antenna will be designed before going to the metamaterial backed design in Section IV. A Coplanar fed Inverted F antenna (CPW-IFA) is selected as the reference antenna for designing the metamaterial backed antenna. A CPW-IFA, as shown in Figure 8can be described as a printed dipole antenna in which one of the dipole arm is bent to form an inverted 'r' shape and the second arm is widened for a larger impedance bandwidth. Due to the high capacitance of the 'r' shape, a shorting strip between the radiating element (the inverted 'r') and the ground plane is placed to compensate for the capacitance. Then the feed is

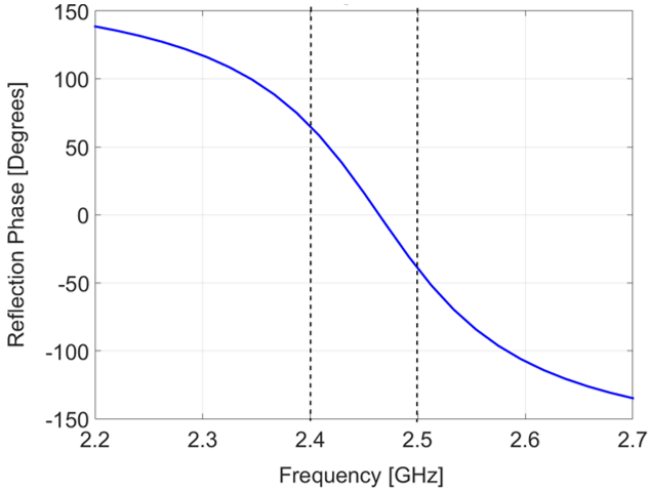

Fig. 7: Phase of the reflected wave on normal incidence to the AMC (HIS plus antenna substrate) (θ= 0; ϕ = 0) under periodic boundary conditions

TABLE I: DIMENSIONS OF CPW-IFA LAYER OF THE REFERENCE AND METAMATERIAL BACKED ANTENNA

mm	Reference Antenna	Metamaterial backed antenna
S_x	60	60
S_y	22	60
g_w	0.5	0.35
T_1	2	2
T_2	9	9
T_3	10	10
L_1	28.2	27.5
L_2	2	2
L_3	26	26
L_4	5	2
L_5	8	10.1

made in a Coplanar wave-guide style. The resulting antenna is compact and has a wider bandwidth than then a conventionally fed IFA antenna. A similar type of antenna was presented in [18] for body-worn applications. Figure 8 shows the CPW-IFA that was designed in this paper. The entire simulation was done using Finite Difference Time domain (FDTD) method in CST Microwave Studio [19]. The substrate thickness was 1.2 mm and the dielectric constant was 2.2. Table I shows the final dimesions of the CPW-IFA, all dimensions are in mm.

The human body is mimicked by using a block of 120 mm×120 mm×17 mm. The properties of the block is set to a conductivity of 1 S/m and a dielectric constant of 42 in CST as proposed in [20]. The CPW-IFA was placed directly on the body model and simulated with no spacing. Figure 9 compares the S_{11} of the antenna with the body model and without model. There is a signficant impedance detuning. The resonant freqency moves far away from the intended 2.45 GHz ISM band to 1.95 GHz. This highlights a challenge of body-worn antennas. Figure 10 shows the gain pattern with and without the body. The gain drops drastically from 2.2 dBi to -8.9 dBi. The radiation efficiency of the antenna drops from 99% to 5%. When a 1 mm spacing is added between the body model and the antenna, the resonant frequency shift is 200 MHz, the gain drops to -6 dBi and the efficiency drops to

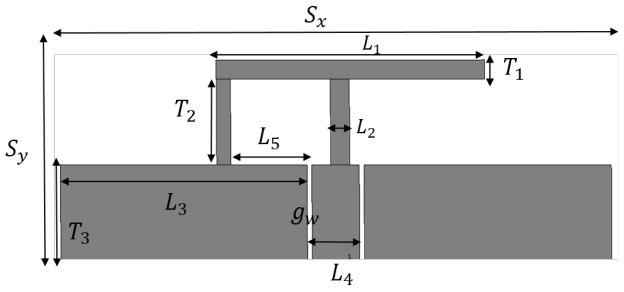

Fig. 8: Reference antenna: CPW-IFA Layout and dimensions

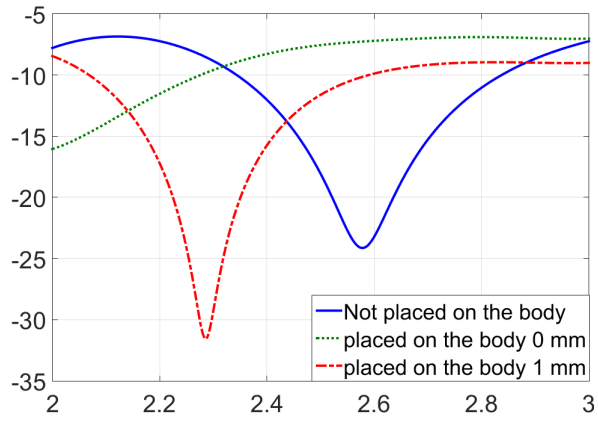

Fig. 9: S_{11} of Reference antenna placed on the body phantom simulated

6.8%. Figure 11 shows the current distribution on the reference antenna.

IV. METAMATERIAL BACKED ANTENNA

A. Design

With the unit cell designed in Section II, a 3×3 array is formed. The top layer of the CPW-IFA designed in Section III is placed on top of the 3×3 array. The AMC is scaled down to a 2×2 array for compactness. The co-planar gap width g_w and the coplanar width L_4 is then used to adjust the S_{11} of the antenna to the 2.45 GHz ISM band. A typical SMA connector width of 4.5 mm is taken into conisderation. The radiation length L_1 and the shorting strip offset L_5 were adjusted as well. Table I shows the final dimensions of the top layer of the AMC backed CPW-IFA antenna. Figure 12 shows the 3 metal layers of the final antenna. The metal layers have a 1.2 mm antenna substrate and 2 mm AMC substrate both of dielectric constant of 4.2 in between them. The total size is 60 mm by 60 mm. the layers were 25 μm thick amounting to a total thickness of 3.275 mm. If a PEC was used instead of the AMC, it would require a total thickness of about 15 mm ($\frac{\lambda/4}{\sqrt{\epsilon_r}}$).

B. Results

Figure 13 shows the 3-D simulation model of the designed antenna on the body phantom block. The entire simulation was

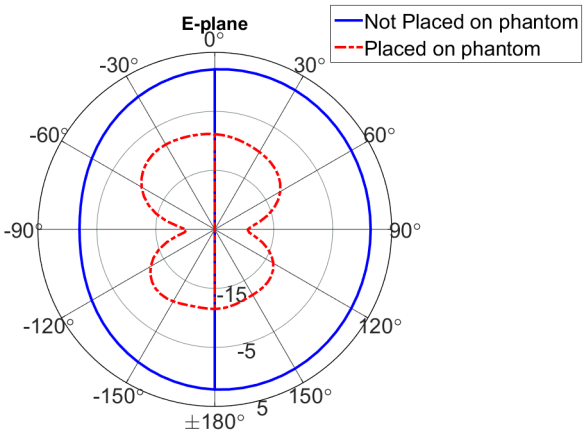

(a) E-plane

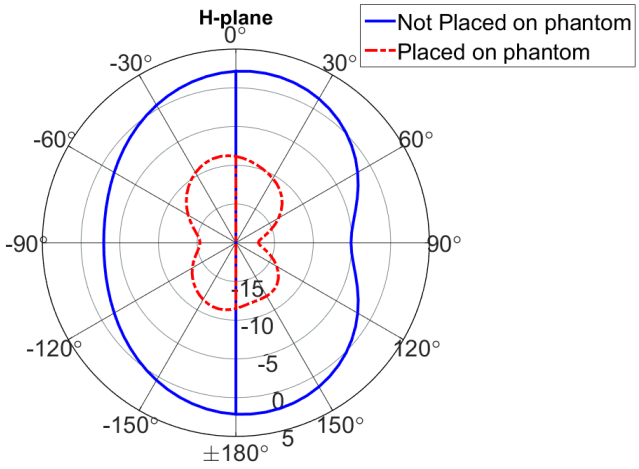

(b) H-plane

Fig. 10: Gain pattern of the reference antenna simulated

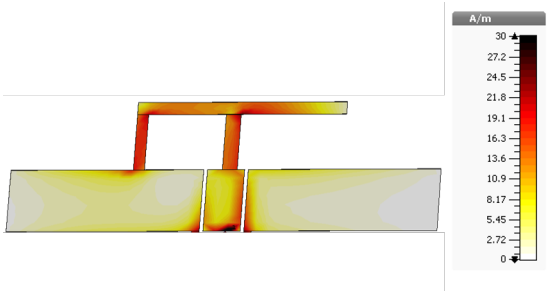

Fig. 11: Surface current distribution on the reference antenna

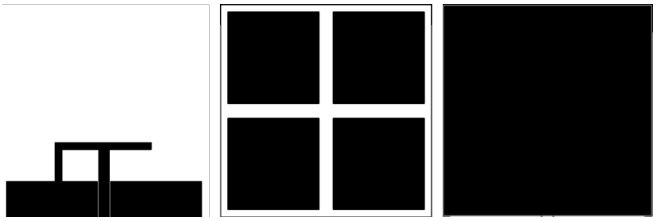

Fig. 12: Metal Layers of the Metamaterial backed antenna

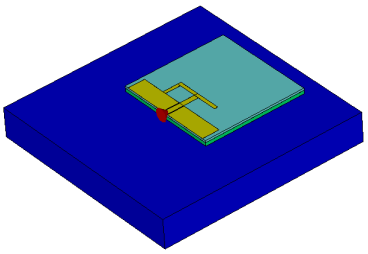

Fig. 13: 3D Simulation model of Designed Antenna on body phantom

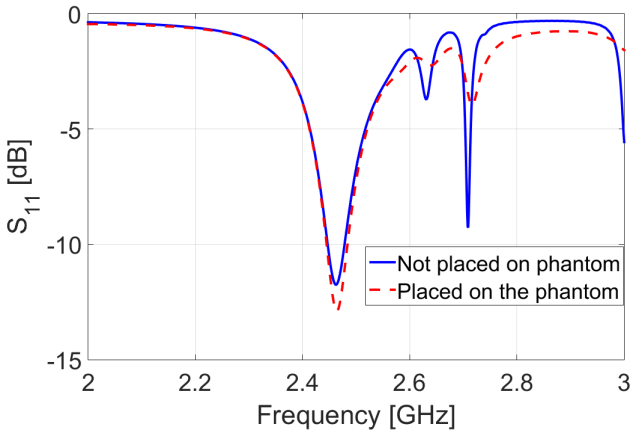

Fig. 14: S_{11} of The designed AMC backed antenna placed on the body phantom simulated

done using FDTD method in CST Microwave Studio. Figure 14 compares the S_{11} of the AMC backed antenna on the body and not placed on the body. The resonant frequency shifted by 3 MHz which is negligible showing the robustness of the metamaterial backed antenna. The 10 dB bandwidth is 50 MHz and the 6 dB bandwidth is 100 MHz. This sufficiently covers the 2.45 GHz ISM band. Figure 15 shows the gain pattern of the antenna with and without body model. The antenna had a good coverage away from the body. The 3dB beamwidth is 88°. The gain of the antenna only drops from 6.5 dBi to 5.7 dBi and the antenna efficiency from 86% to 71%. Figure 16 shows the surface current distribution on the metal layers of the antenna.

C. Comparison with reference antenna

Table II compares the performance of the metamaterial backed antenna and that of the reference antenna. For a stricter comparison, the reference antenna is placed 1 mm away from the body to compensate the fact that the metamaterial backed antenna is 2 mm thicker and hence $2/\epsilon_r$ electrically thicker. The metamaterial backed antenna is clearly more robust to impedance detuning even though its bandwidth was less than that of the reference antenna. The AMC back antenna provides sufficient gain, efficiency and radiation away from the body in contrast to the reference antenna.

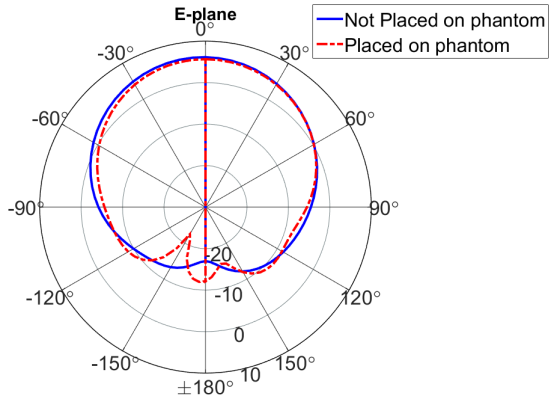

(a) E-plane

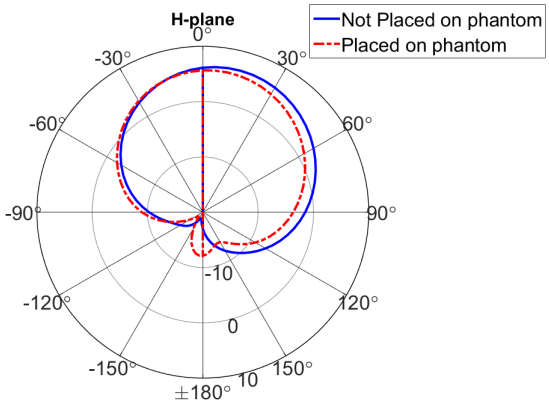

(b) H-plane

Fig. 15: Gain pattern of the AMC backed antenna simulation

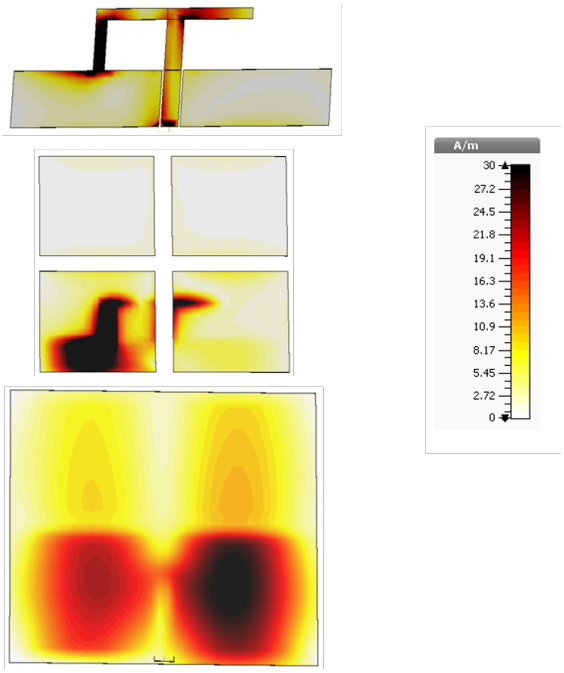

Fig. 16: Surface current distribution on the Metamaterial backed antenna

TABLE II: COMPARING REFERENCE AND METAMETERIAL AMC BACKED ANTENNAS

	CPW-IFA	AMC CPW-IFA
Gain [dBi]	2.2	6.5
Gain (on the body) [dBi]	-8.9	5.7
Gain (on body) 1 mm [dBi]	-6	
Efficiency [%]	99	86
Efficiency (on the body) [%]	5	71
Efficiency (on the body) 1 mm [%]	6.8	
Resonance Frequency shift [MHz]	500	3
Resonance Frequency shift 1 mm [MHz]	200	
Bandwidth [MHz]	500	50
Front to back radiation ratio	2.6	24

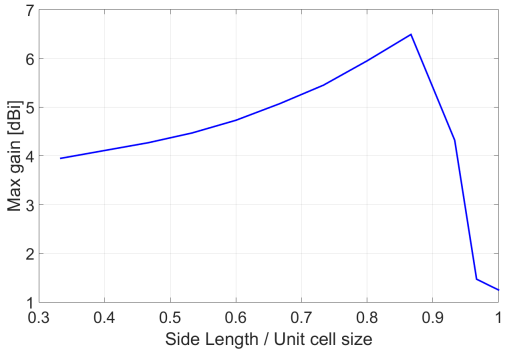

Fig. 17: Gain vs side length of the metallic patches

V. PARAMETRIC ANALYSIS

In this section, key parameters are varied such as the size of the metallic patches of the AMC, the AMC array size and the position of the antenna layer on its AMC backing. This gives insights to their sensitivity, operation, and variants of the design.

A. Varying the size of the metallic patches of the AMC

The side length of the metallic square patches is varied between 10 mm to 30 mm with the unit cell size remaining 30 mm (recall Figure 4a). This corresponds to a side length to unit cell size ratio of 0.33 - 1.00. Figure 17 shows the gain of the antenna against the side length of the metallic patches of the AMC. Figure 18 shows the reflection phase diagram at various side lengths. The maximum gain occurs at ratio 0.867 which is the same the side length where the structure is in the AMC region around the 2.45 GHz ISM band.

B. Varying the array size of the AMC

The AMC backing array size is varied from 2×2 to 3×3 and 1×2 (see Figure 19). Table III shows the directivity and gain of the antenna when backed by each array size. The 2×2 is optimal since it is compact and has a gain comparable to the 3×3. The efficiency of the 1×2 array backing is lowest due to less the AMC backing it radiating element at the top layer experiences.

C. Varying the position of the CPW-IFA layer on the AMC

The position of the antenna layer is varied across its plane on a 3×3 AMC backing. Figure 20 shows the antenna layer

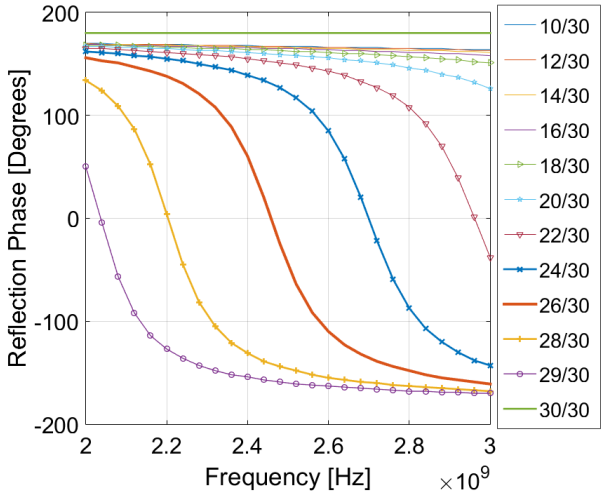

Fig. 18: Reflection phase at various side length to unit cell size ratio

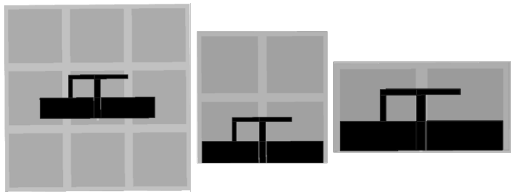

Fig. 19: CPW-IFA on various AMC array sizes

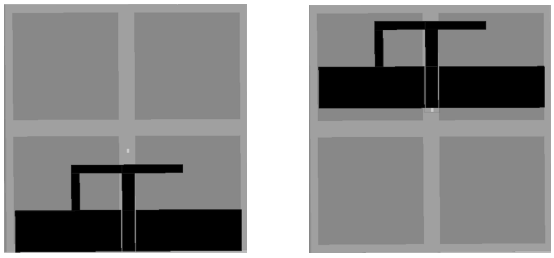

(a) Antenna shift = 0 mm (b) Antenna Shift = 35 mm

Fig. 20: Antenna at two extreme positions

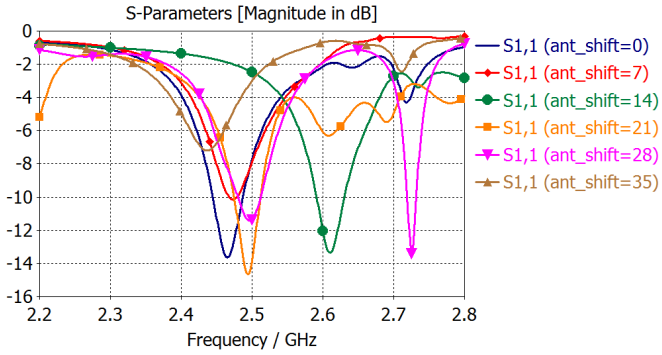

Fig. 21: S_{11} on phantom: antenna over position on its AMC Backing

at 2 extreme positions that were simulated. The first one has no offset while the other was an offset of 35 mm. Figure 21 shows S_{11} at various offset positions. The resonant frequency shifts by a maximum of 5%. The resonant frequency could easily be turned to be at 2.45 GHz using the gap width and thickness of the coplanar feeding at the antenna layer. Figure 22 shows the maximum gain at various positions. The gain of the antenna is insensitive to its position above the AMC backing as long as it is not close to an edge. However when radiating element on the CPW-IFA is very close to the edge, the gain reduces. This is due to that the radiating element sees less AMC backing.

VI. Fabrication and Measurements

Figure 23 shows a picture of the fabricated AMC backed CPW-IFA. The metamaterial backed antenna was manufactured using a IS420 substrate which has a dielectric constant 4.04 and a loss tangent of ~ 0.015. Its loss tangent is quite high compared to the simulated low loss tangent of 0.002 but its dielectric constant is very close to the simulated antenna. The top copper layer (the CPW-IFA) and the antenna substrate was bonded to the last 3 layers which is the AMC backing consisting of the 2 by 2 array of copper patches, the AMC substrate and copper plane. It is bonded using a prepreg material of the IS420 substrate. The metal layers are finished with a tin coating for durability. An SMA connector was soldered to the antenna. The antenna has no grounding vias and no connection to the bottom, which is the metal plane.

The S_{11} was measured and compared against the default FDTD simulation used throughout the paper, and an additional Finite Element Method (FEM) Simulation in CST. Figure 25 shows the S_{11} result. Measurement and simulation are close:

TABLE III: Performance at various AMC array size

	Eff.(w/ body)	Eff.	Gain (w/body)	Gain	Dir.
3x3	68.0%	74.2%	5.30 dBi	5.03 dBi	6.33 dBi
2x2	70.7%	86.3%	5.72 dBi	6.49 dBi	7.13 dBi
1x2	58.1%	87.6%	4.63 dBi	5.14 dBi	5.71 dBi

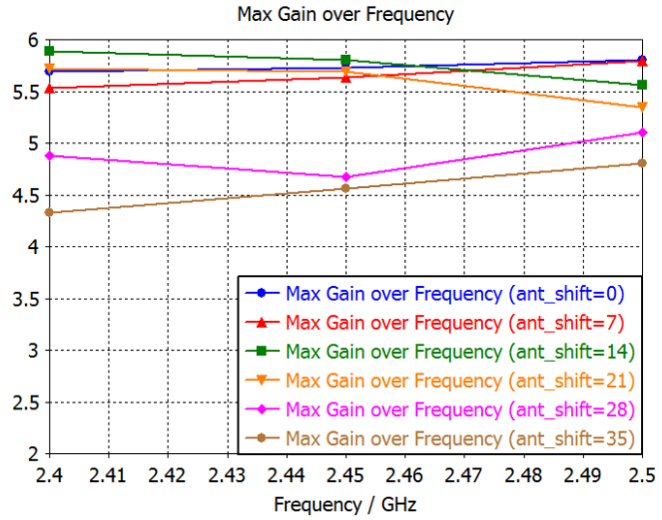

Fig. 22: Gain of antenna over position on its AMC Backing

there is a 40 MHz difference in the resonant frequency with the FDTD simulation which comes from SMA connector connection and the dielectric constant of the substrate. Figure 26 compares the gain pattern of the simulated and the measured antenna. The radiation pattern simulation results match well with the measurements. The antenna has a 3-dB beamwidth of 87° and 85° in the E-plane and H-plane respectively. The beam is concentrated away from the body and still provides good coverage. The measured antenna has a gain of 4.2 dBi which is 2.3 dB lower than the simulation. This is due to the higher loss tangent of the IS420 substrate that has a loss tangent of 0.015 in contrast to a low tangent of 0.002 used in simulation.

For the antenna-on-body measurements, a tissue simulating liquid mainly consisting of DGBE (Diethylene glycol butyl ether), and water was used in a 0.85 L container. Figure 24 shows the antenna on the container filled with the tissue simulating liquid. The liquid was obtained from Schmid & Partner Engineering AG and conforms to FCC KDB 865664 standard. A similar tissue simulation liquid was manufactured in [21]. As in the simulation, the resonant frequency of the antenna had a minor shift of less than 5 MHz when placed on the body phantom. The gain dropped slightly from 4.2 dBi to 3.4 dBi when placed on the phantom.

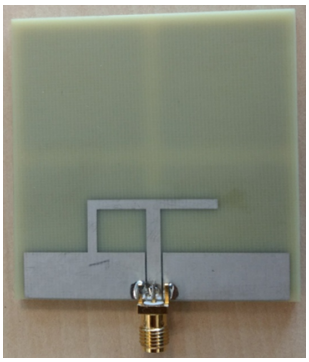

Fig. 23: The fabricated metamaterial backed antenna

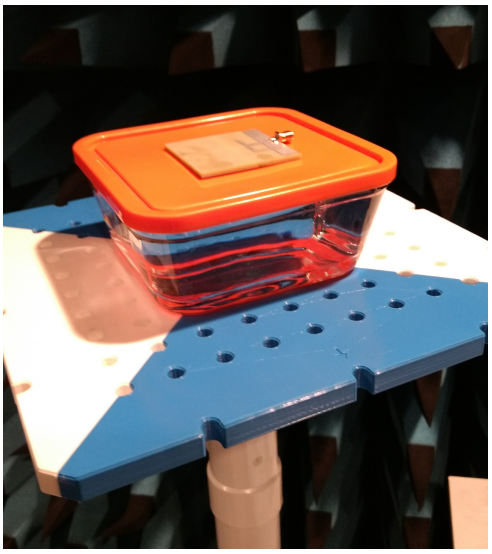

Fig. 24: Fabricated Antenna on the phantom

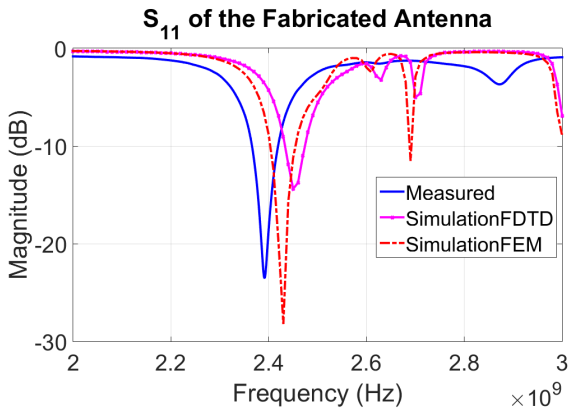

Fig. 25: S_{11} of the fabricated antenna

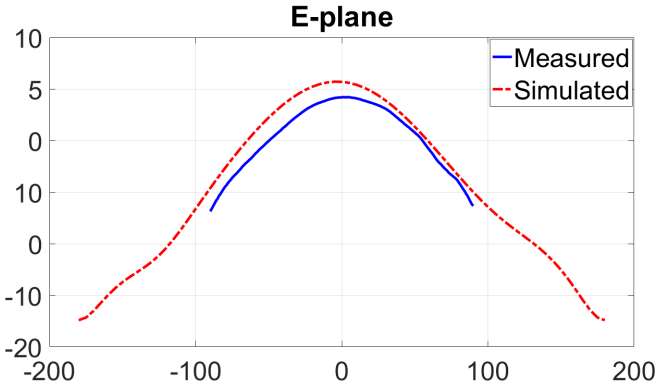

(a)

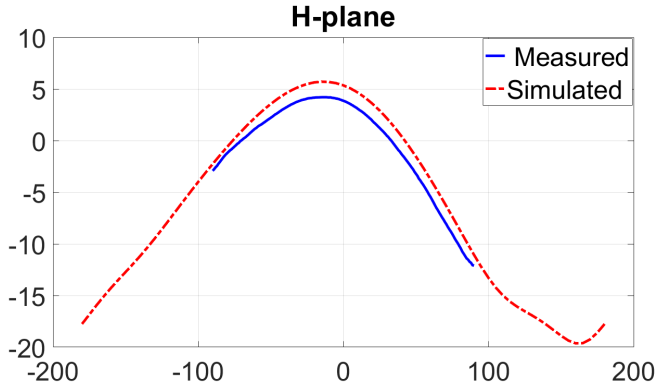

(b)

Fig. 26: Gain pattern of the AMC backed CPW-IFA

VII. Conclusions and Recommendations

In this paper, a metamaterial backed body-worn antenna comprising of a CPW-IFA and an AMC backing, targeted for receiver off-body communication was designed, simulated and fabricated. The antenna is fairly compact having a total size of 60 mm×60 mm×3.28 mm. The AMC backing shielded the antenna from being degraded by the human body while maintaining good input matching. If a PEC was used instead of the AMC, it would require a substrate thickness of about 15 mm. Although the simulated 10 dB bandwidth of the AMC backed CPW-IFA was 50 MHz compared to 500 MHz of the

reference antenna, the AMC backed CPW-IFA was robust to impedance detuning when placed directly on the body showing only 3 MHz shift compared to the 500 MHz shift experienced in the reference antenna. The designed antenna had a drop in gain when placed on the body of only 0.8 dB compared to the more than 10 dB drop in gain the body-worn CPW-IFA. The efficiency of the designed antenna on the body was 71% compared to 5% efficiency of the body-worn CPW-IFA . The measured radiation pattern showed that the fabricated antenna has a good coverage away from the body and minimal radiation towards the body with a 3dB beamwidth of 88°. The designed novel antenna is suitable for integration with electronics thereby building body-worn devices with good off-body communication performance.

In the future exploring flexible substrates with low loss tangent (< 0.002) would be useful to achieve the simulated gain of 6.5 dBi. Although the antenna is fairly compact, evaluating antenna performance when a bent at various angles could be also interesting to explore.

ACKNOWLEDGMENT

The author would like to thank Ir. M. Kleijnen and Ir. G. Doodeman of Philips for their technical assistance. The author would also like to appreciate Asst. Prof. V. Lancellotti for his support and critical comments.

REFERENCES

[1] P. Hall and Y. Hao, *Antennas and Propagation for Body-Centric Wireless Communications*, 2nd ed. Artech House, 2012.

[2] G. Conway, W. Scanlon, and A. Chandran, "Antennas for over-body-surface communication at 2.45 ghz," *IEEE Transactions on Antennas and Propagation*, vol. 57, no. 4, pp. 844–855, 2009.

[3] D. R. Smith, W. J. Padilla, D. C. Vier, S. C. Nemat-Nasser, and S. Schultz, "Composite medium with simultaneously negative permeability and permittivity," *Phys. Rev. Lett.*, vol. 84, pp. 4184–4187, May 2000.

[4] F.-R. Yang, K.-P. Ma, Y. Qian, and T. Itoh, "A uniplanar compact photonic-bandgap (uc-pbg) structure and its applications for microwave circuit," *IEEE Transactions on Microwave Theory and Techniques*, vol. 47, no. 8, pp. 1509–1514, Aug 1999.

[5] B. Munk, *Frequency Selective Surfaces: Theory and Design*. Wiley, 2000.

[6] D. Sievenpiper, L. Zhang, R. Broas, N. Alexopolous, and E. Yablonovitch, "High-impedance electromagnetic surfaces with a forbidden frequency band," *IEEE Transactions on Microwave Theory and Techniques*, vol. 47, no. 11, pp. 2059–2074, 1999.

[7] D. J. Kern, D. H. Werner, A. Monorchio, L. Lanuzza, and M. J. Wilhelm, "The design synthesis of multiband artificial magnetic conductors using high impedance frequency selective surfaces," *IEEE Transactions on Antennas and Propagation*, vol. 53, no. 1, pp. 8–17, Jan 2005.

[8] P. Salonen, "A low-cost 2.45 ghz photonic band-gap patch antenna for wearable systems," *11th International Conference on Antennas and Propagation (ICAP 2001)*, 2001.

[9] R. Gonzalo, P. De Maagt, and M. Sorolla, "Enhanced patch-antenna performance by suppressing surface waves using photonic-bandgap substrates," *IEEE Transactions on Microwave Theory and Techniques*, vol. 47, no. 11, pp. 2131–2138, 1999.

[10] X. yu Li, J. Li, J. jun Tang, X. liang Wu, and Z. xiang Zhang, "High gain microstrip antenna design by using fss superstrate layer," in *2015 4th International Conference on Computer Science and Network Technology (ICCSNT)*, vol. 01, Dec 2015, pp. 1186–1189.

[11] A. Feresidis, G. Goussetis, S. Wang, and J. Vardaxoglou, "Artificial magnetic conductor surfaces and their application to low-profile high-gain planar antennas," *IEEE Transactions on Antennas and Propagation*, vol. 53, no. 1, pp. 209–215, 2005.

[12] Y. Fan Yang, Rahmat-Samii, "Reflection phase characterizations of the ebg ground plane for low profile wire antenna applications," *IEEE Transactions on Antennas and Propagation*, vol. 51, no. 10, pp. 2691–2703, 2003.

[13] P. Salonen, M. Keskilammi, J. Rantanen, and L. Sydanheimo, "A novel bluetooth antenna on flexible substrate for smart clothing," *IEEE International Conference on Systems, Man and Cybernetics. e-Systems and e-Man for Cybernetics in Cyberspace (Cat.No.01CH37236)*, 2001.

[14] M. E. de Cos and F. Las-Heras, "Polypropylene-based dual-band cpw-fed monopole antenna [antenna applications corner]," *IEEE Antennas and Propagation Magazine*, vol. 55, no. 3, pp. 264–273, June 2013.

[15] Y. Liu, QingshuangLu, "Cpw-fed wearable textile l-shape patch antenna," *Proceedings of 2014 3rd Asia-Pacific Conference on Antennas and Propagation*, 2014.

[16] D. F. Sievenpiper, "High-impedance electromagnetic surfaces," Ph.D. dissertation, University of Carlifornia, 1999.

[17] [Online]. Available: http://www.feko.info/

[18] A. Abbosh, H. Al-Rizzo, S. Abushamleh, A. Bihnam, and H. R. Khaleel, "Flexible cpw-ifa antenna for wearable electronic devices," *2014 IEEE Antennas and Propagation Society International Symposium (APSURSI)*, 2014.

[19] [Online]. Available: https://www.cst.com/

[20] M. Rutschlin, "Simulation of wearable antennas for body centric wireless communication," *CST Webinar 2013*, December 2013.

[21] T. Yilmaz, T. Karacolak, and E. Topsakal, "Characterization and testing of a skin mimicking material for implantable antennas operating at ism band (2.4 ghz-2.48 ghz)," *IEEE Antennas and Wireless Propagation Letters*, vol. 7, pp. 418–420, 2008.

[22] P. Salonen, F. Yang, Y. Rahmat-Samii, and M. Kivikoski, "Webga - wearable electromagnetic band-gap antenna," *IEEE Antennas and Propagation Society Symposium, 2004.*, vol. 1, pp. 451–454, 2004.

[23] B. Farooq, T. Parveen, I. Ali, and S. Ullah, "Antenna design for advance wireless systems using metamaterial surfaces," *2016 13th International Bhurban Conference on Applied Sciences and Technology (IBCAST)*, 2016.

[24] H. Yang, S. Chen, Q. Zhang, and W. Zheng, *Analysis of a Novel Electromagnetic Bandgap Structure for Simultaneous Switching Noise Suppression*. Berlin, Heidelberg: Springer Berlin Heidelberg, 2011, pp. 628–634.

[25] T. Kellomaki, W. G. Whittow, J. Heikkinen, and L. Kettunen, "2.4 ghz plaster antennas for health monitoring," in *2009 3rd European Conference on Antennas and Propagation*, March 2009, pp. 211–215.

[26] A. M. E. El-sheakh, Dalia M.Safwat, "Multi-band cpw- fed printed ifa," *Proceedings of the 2012 IEEE International Symposium on Antennas and Propagation*, 2012.

[27] A. Bhattacharya, "Modelling metamaterials," *Physics' Best*, 2014.

[28] D. M. Elsheakh and E. A. Abdallah, "Multiband printed-ifa on electromagnetic band-gap ground plane," in *Proceedings of the 2012 IEEE International Symposium on Antennas and Propagation*, July 2012, pp. 1–2.

[29] J. C. Vardaxoglou, A. P. Feresidis, and G. Goussetis, "Recent advances on ebg and amc surfaces with applications in terminal and high gain antennas," in *TELSIKS 2005 - 2005 uth International Conference on Telecommunication in ModernSatellite, Cable and Broadcasting Services*, vol. 1, Sept 2005, pp. 3–6 vol. 1.

[30] P. Bhartia, I. Bahl, R. Garg, and A. Ittipiboon, *Microstrip Antenna Design Handbook*. Artech, 2001.

[31] C. Hertleer, H. Rogier, L. Vallozzi, and L. V. Langenhove, "A textile antenna for off-body communication integrated into protective clothing for firefighters," *IEEE Transactions on Antennas and Propagation*, vol. 57, no. 4, pp. 919–925, April 2009.

[32] A. R. Chandran, G. A. Conway, and W. G. Scanlon, "Pattern switching compact patch antenna for on-body and off-body communications at 2.45 ghz," in *2009 3rd European Conference on Antennas and Propagation*, March 2009, pp. 2055–2057.

[33] B. Woods, "Design and analysis of antennas for a modern smartwatch," *CST Smatch Watch Webinar 2016*, September 2016.

[34] B. Rana, A. Chatterjee, and S. K. Parui, "Gain enhancement of a direct microstrip line fed dielectric resonator antenna using fss," in *2015 IEEE Applied Electromagnetics Conference (AEMC)*, Dec 2015, pp. 1–2.

[35] P. Salonen, L. Sydanheimo, M. Keskilammi, and M. Kivikoski, "A small planar inverted-f antenna for wearable applications," in *Wearable Computers, 1999. Digest of Papers. The Third International Symposium on*, 1999, pp. 95–100.